International Journal of Mass Spectrometry 273 (2008) 126–131

Contents lists available at ScienceDirect

International Journal of Mass Spectrometry

journal homepage: www.elsevier.com/locate/ijms

On the formation and fragmentation of nitrate in mixed clusters using atmospheric pressure corona discharge in air

Kasper Drenck, Preben Hvelplund*, Steen Brøndsted Nielsen, Subhasis Panja, Kristian Støchkel

Department of Physics and Astronomy, University of Aarhus, Ny Munkegade, DK-8000 Aarhus C, Denmark

ARTICLE INFO

Article history:
Received 12 February 2008
Received in revised form 25 March 2008
Accepted 25 March 2008
Available online 10 April 2008

Keywords:
Corona discharge
Negative ion hydration
Charge reversal
CID

ABSTRACT

We report on studies of NO_3^- in mixed clusters of HNO_3 and H_2O, $NO_3^-(HNO_3)_m(H_2O)_n$ with $m = 0–3$ and $n = 0–300$. The ions were formed in a corona discharge in ambient air in the point to plane configuration and investigated in a sector type mass spectrometer. The yields of individual ions depend strongly on the shape of the needle and the needle voltage. An STM needle with a tip radius of around 20 nm, resulted in clusters with $m = 2$ and 3 and n around 100. After collision-induced dissociation (CID) at 50 keV with Ne gas both positive and negative fragment ions were recorded and unambiguous information about the cluster composition was obtained. Density functional theory (DFT) calculations have been employed to shed light on the experimental findings.

1. Introduction

Ion-induced nucleation is believed to be an important first step towards the formation of aerosols in the Earth's atmosphere [1–3]. Both positive and negative ions act as nucleation centers but negative ions in particular are believed to be important for ion–molecule reactions and cluster formation processes. It has thus been shown by Svensmark et al. [4] that under experimental conditions similar to those found in the lower troposphere the production of aerosol particles is proportional to the negative ion density. Svensmark [5] also argues that variations in the ion density in the Earth's atmosphere are caused by variation of the intensity of galactic cosmic rays. This variation in turn is argued to be due to changes in the solar magnetic activity. A better understanding of the first steps from core ion production to nanosolvation of these ions is absolutely crucial for this scenario, where the last step is cloud formation.

In recent experiments [6–8] it has been demonstrated that the core ion NO_3^- plays an important role as a nucleation center for cluster growth in experiments where a corona discharge ion source is coupled to a mass spectrometer. In particular it was found that cluster ions as $NO_3^-(HNO_3)_n$ and $NO_3^-(H_2O)_m$ are final products in the nucleation process. Both reaction times and corona needle voltage were found to have a strong influence on relative ion intensities in the recorded mass spectra. These findings can be associated to differences in rates for ion molecule reactions and differences in ion stability. The chemical reactions taking place in a corona discharge is also found to be relevant for various nitrogen fixation schemes [9]. The production of nitric acid from air by arcing is known as the Birkeland–Eyde process.

In the present study the corona discharge is taking place between a needle and a heated capillary that acts as an entrance to the vacuum region. This capillary is normally used as the interface between the spray needle and the accelerator mass spectrometer when the ions are produced by electrospray ionization (ESI) [10]. We demonstrate that the recorded anion mass spectra are strongly influenced by needle shape, needle voltage and heated capillary temperature. Using this technique we show that several hundreds of water molecules cluster to the negative core ions.

2. Experimental

The experimental arrangement is described in detail in [10] and shown schematically in Fig. 1. The ions were in the present experiment formed by corona discharge in ambient air. The corona ionizer is shown in Fig. 2. It consists of a discharge needle and the heated capillary normally used as the interface in our electrospray ion source. The temperature of the heated capillary can be varied between room temperature and 200 °C. The distance between the needle tip and the entrance end of the heated capillary was 3 mm. The heated capillary is made from stainless steel and is 10 cm long with an inner diameter of 0.4 mm. The pressure varies through the capillary from atmospheric pressure at the entrance to around 1 mbar at the exit end. The time it takes the ions to pass through the capillary is estimated to be around 1.5 ms based on air flow

* Corresponding author.
E-mail address: hvelplun@phys.au.dk (P. Hvelplund).

1387-3806/$ – see front matter © 2008 Elsevier B.V. All rights reserved.
doi:10.1016/j.ijms.2008.03.014

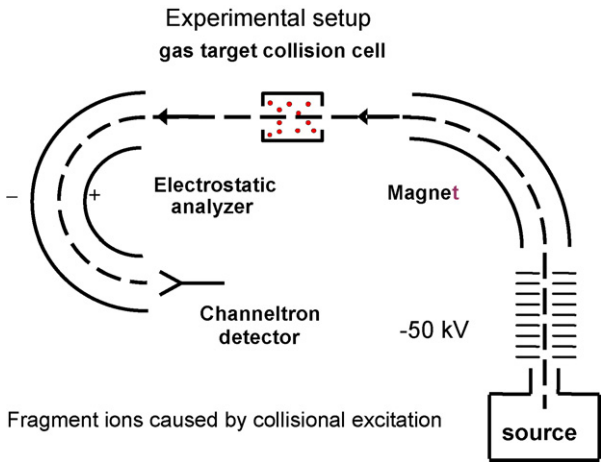

Fig. 1. Overview of the experimental setup.

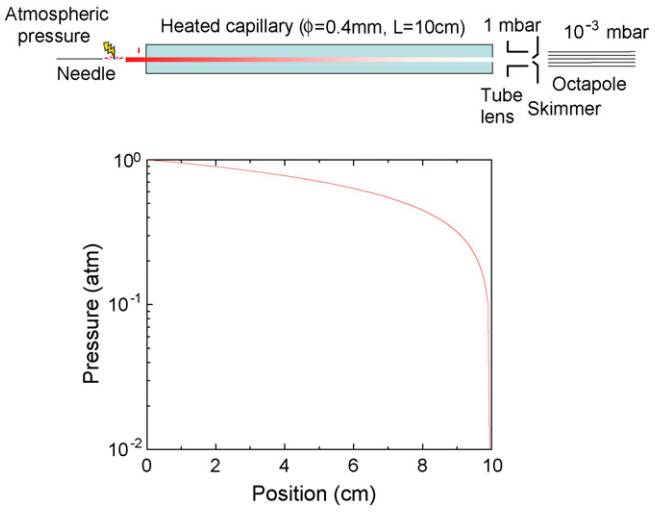

Fig. 2. Schematic illustration of the corona discharge ion source. The graph shows the pressure drop through the heated capillary.

measurements. Two different discharge needles were used in this experiment. One was a normal sewing needle and the other was a special scanning tunnel microscopy (STM) needle (Kentax UHV-Components, Billerbeck, Germany) made from tungsten. This STM needle was 3 mm long with a diameter of 0.3 mm. An electron microscopy picture of a fresh and a used needle is shown in Fig. 3. This picture was taken by a scanning electron microscope (FEGSEM Nova 600 from FEI). From a picture of the needle with a much higher resolution the radius of curvature of the tip is estimated to be around 20 nm. The corona voltage was between 2 and 3 kV, the tube lens potential was 60 V and the heated capillary temperature was normally held at room temperature. The ions were accelerated by an electrostatic potential of 50 kV. The precursor ions were mass selected with a bending magnet and passed through a 3-cm long gas cell with entrance and exit apertures of 1 and 3 mm diameter containing neon as target gas. The Ne target gas pressure was monitored by a cold cathode gauge. The product ions exiting the cell were analyzed according to their m/z, by scanning the voltage of the electrostatic hemispherical analyzer and fragmentation spectra were obtained. Mass spectra showing the distribution of ions produced in the ion source were obtained by scanning the magnet with no target gas in the target cell and using a fixed analyzer voltage that was related to the acceleration voltage.

3. Computational details

Geometries of $NO_3^-(HNO_3)_m(H_2O)_n$, H_2O, and HNO_3 were optimized at the B3LYP/6–31++G(d,p) level of theory and vibrational frequencies were calculated using the Gaussian-98 program package [11]. Electronic energies corrected for zero-point kinetic energies were used to calculate complexation energies, defined as the energy gained in the reaction,

$$NO_3^- + mHNO_3 + nH_2O \rightarrow NO_3^-(HNO_3)_m(H_2O)_n$$

4. Experimental results and discussion

Both ozone and nitrogen oxides are produced in the corona discharge. Nitric oxide (NO) is formed from nitrogen and oxygen atoms produced by electron impact dissociation [6]. NO_2 is then produced by oxidation of NO. Skalny et al. [6] also argue that NO_3^- ions are most likely formed in the reaction

$$CO_3^- + NO_2 \rightarrow CO_2 + NO_3^-$$

Atkinson et al. [12] propose, HNO_3 to be formed in the reaction

$$NO_2 + OH + M \rightarrow HNO_3 + M,$$

where M is a collider.

Since ambient air with a relative humidity of around 50% was used in our experiments, a large number of H_2O molecules were

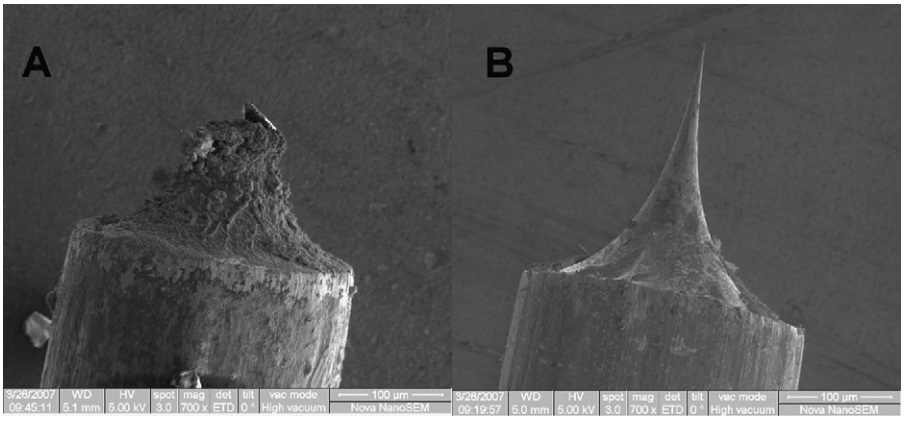

Fig. 3. Electron microscope pictures of the STM needle used for corona discharge, (A) after use for several hours and (B) before use.

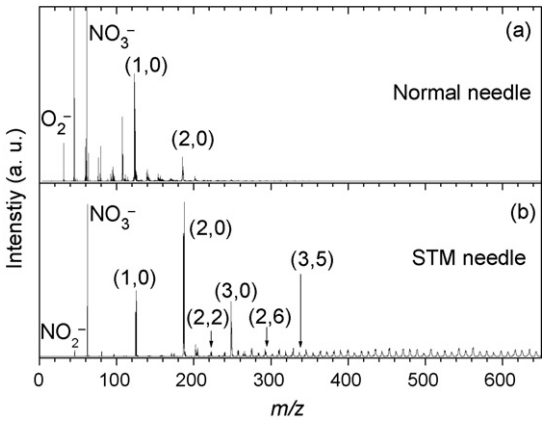

Fig. 4. Negative ion mass spectra where the corona discharge took place in ambient air, (a) with a sewing needle and (b) with the STM needle.

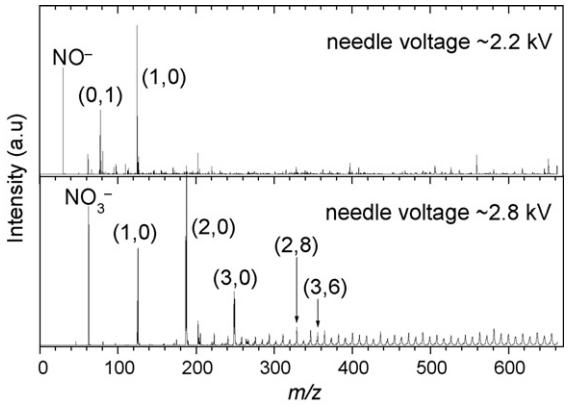

Fig. 6. Negative ion mass spectra obtained with an STM needle at two different needle voltages.

present in the reaction zone. Nagato et al. [7] argue that HCO_3^- is formed in ambient air in the reaction.

$$OH^- + CO_2 + M \rightarrow HCO_3^- + M$$

The building blocks for the mixed clusters around the core ions NO_3^- and HCO_3^- are thus available and clusters of the type $NO_3^-(HNO_3)_m(H_2O)_n$ or $HCO_3^-(HNO_3)_m(H_2O)_n$ can readily be formed under optimal experimental conditions. Fig. 4 shows mass spectra of ions formed by corona discharge in ambient air with two different corona needles. The nomenclature (m,n) denotes $NO_3^-(HNO_3)_m(H_2O)_n$. More $NO_3^-(HNO_3)_3$ and $HCO_3^-(HNO_3)_3$ ions are produced when using the STM needle as compared to the normal needle but even more striking is that these ions are much more likely to be hydrated. The relative intensity of ions with 20–30 water molecules attached is 10 times higher with the STM needle than with the normal needle. This could indicate that at least some solvation takes place in the discharge region but it cannot be ruled out that further water addition occurs in the expansion region after the capillary. A magnet scan recorded with an STM needle at a corona voltage of 2.8 kV is depicted in Fig. 5. The mass range extends up to 4200 Da corresponding to a core ion solvated by around 200 water molecules. It is noted that the spectrum consists of peaks separated by 9 Da. It is also readily observed that the spectrum shows two series of independent ions. Since the nominal

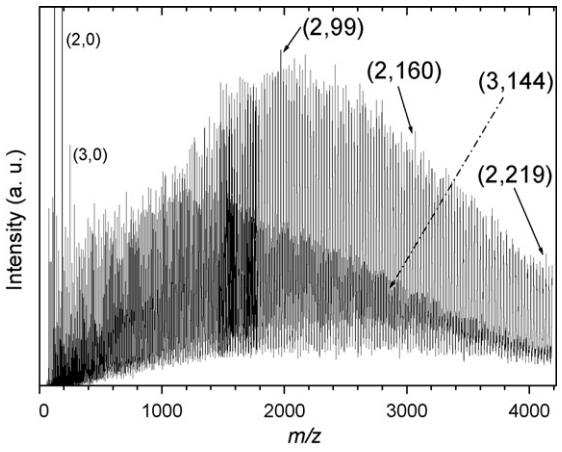

Fig. 5. Negative ion mass spectrum where the corona discharge took place in ambient air. The spectrum is dominated by the two series of solvated ions that can be ascribed to $NO_3^-(HNO_3)_2(H_2O)_n$ and $NO_3^-(HNO_3)_3(H_2O)_n$, respectively. Note that the mass peaks are separated by 9 Da since the mass of seven water molecules is the same as the mass of two nitric acid molecules.

molecular weight of two HNO_3 molecules is equal to that of seven H_2O molecules, we conclude that the two series originate from two core ions where one contains one more HNO_3 than the other. From a closer inspection of ions at low masses it is concluded that the two series correspond to ions of the two types $NO_3^-(HNO_3)_2(H_2O)_n$ and $NO_3^-(HNO_3)_3(H_2O)_n$. It appears that the first series peaks at a mass around 2000 Da while the other peaks at around 1000 Da. The fall to the right of the peak can be accounted for by a combination of rest gas collision and unimolecular decay. This implies that also very large hydrated ions are formed in the first place but that they decay before they reach the detector. There must of course be an upper limit to the size of the mixed clusters since a limited number of interactions with water molecules take place in the ion source.

Two mass spectra recorded at needle voltages of 2.2 and 2.8 kV are shown in Fig. 6. More nitric acid and more water molecules are bound to the core ion NO_3^- at the highest needle voltage. This may suggest that the ion molecule chemistry taking place in the corona discharge is strongly influenced by the electric field strength near the needle tip. It has earlier been shown by Sekimoto and Takayama [8] that the formation of various core ions depends strongly on the needle voltage. In their experiment the OH^- was dominating at low needle voltages and HNO_3^- at high needle voltages. It appears from Fig. 6 that the maximum number of nitric acid molecules included in the mixed clusters is 3 but mass-analyzed ion kinetic energy (MIKE) spectra obtained with a beam that could be a mixture of $NO_3^-(HNO_3)_4$ and $NO_3^-(HNO_3)_2(H_2O)_7$ (not shown) indicate that $NO_3^-(HNO_3)_4$ is formed in our experiments. It should also be mentioned that Shindler et al. [13] have observed $NO_3^-(HNO_3)_4$ ions as a result of reactions between negative cluster ions and chlorine nitrate but that larger clusters were not clearly observed.

In order to better understand these findings, we have calculated complexation energies of $NO_3^-(HNO_3)_m(H_2O)_n$ clusters at the B3LYP/6–31++G(d,p) level of theory, that is, the total energy (at 0 K) required to dissociate a cluster into bare NO_3^-, m HNO_3 and n H_2O (Fig. 7). Values for $NO_3^-(H_2O)$ and $NO_3^-(H_2O)_2$ are 0.61 and 1.13 eV in good agreement with experimental enthalpies of 0.63 and 1.25 eV reported by Lee et al. [14]. The enthalpy changes for loss of HNO_3 from $NO_3^-(HNO_3)_2$ and $NO_3^-(HNO_3)_3$ have been measured to 0.77 and 0.69 eV [14], which is again well reproduced by the calculations (0.77 and 0.66 eV, respectively). The theoretical model therefore seems appropriate to handle these ionic clusters. However, due to computational limitations and the many possible structures of large clusters, the ions under study contained a maximum of six solvent molecules ($m + n = 6$). Optimized structures are given in Fig. 8. It is evident from Fig. 7 that a purely hydrated ion has the lowest complexation energy whereas clusters of only

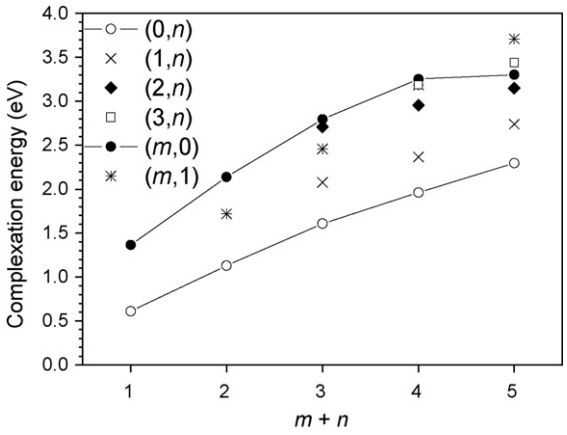

Fig. 7. Calculated complexation energies for $NO_3^-(HNO_3)_m(H_2O)_n$ for $m+n<6$, calculated at the B3LYP/6–31++G(d,p) level of theory. Points are connected with lines for clusters of either nitric acid or water, $NO_3^-(HNO_3)_m$ and $NO_3^-(H_2O)_n$.

HNO_3 are preferential for $m=1$–3. This is explained from a larger dipole moment as well as polarizability of HNO_3 relative to H_2O. The complexation energy of (4,0) is similar to that of (3,1) whereas the complexation energy of (5,0) is less than those of (4,1) and (3,2). Hence for larger cluster sizes than four, it is energetically favorable to include at least one water molecule in the complex. Water allows for a more extended hydrogen bond network that stabilizes the complex by more than is lost from the lower ion–dipole and ion-induced dipole interaction energies. Finally, exchange of HNO_3 for H_2O in $NO_3^-(HNO_3)_m$ is entropically favored by $RT\ln(m)$ [15]; for $m=5$ and $T=298$ K this number is 0.04 eV. In conclusion, particularly stable supramolecular complexes are formed by incorporation of water in the HNO_3 cluster, e.g., the (3,3) structure in Fig. 8, which provides an explanation for the experimental finding of a low yield of clusters with a large number of nitric acids.

Reactions between positive water cluster ions and nitric acid vapor have been studied by Castleman and coworkers [16]. The reactions took place in a flow tube and mixed clusters of the type $D^+(DNO_3)_m(D_2O)_n$ were observed. Deuterium atoms were used for experimental reasons. Incorporation into the water clusters of a

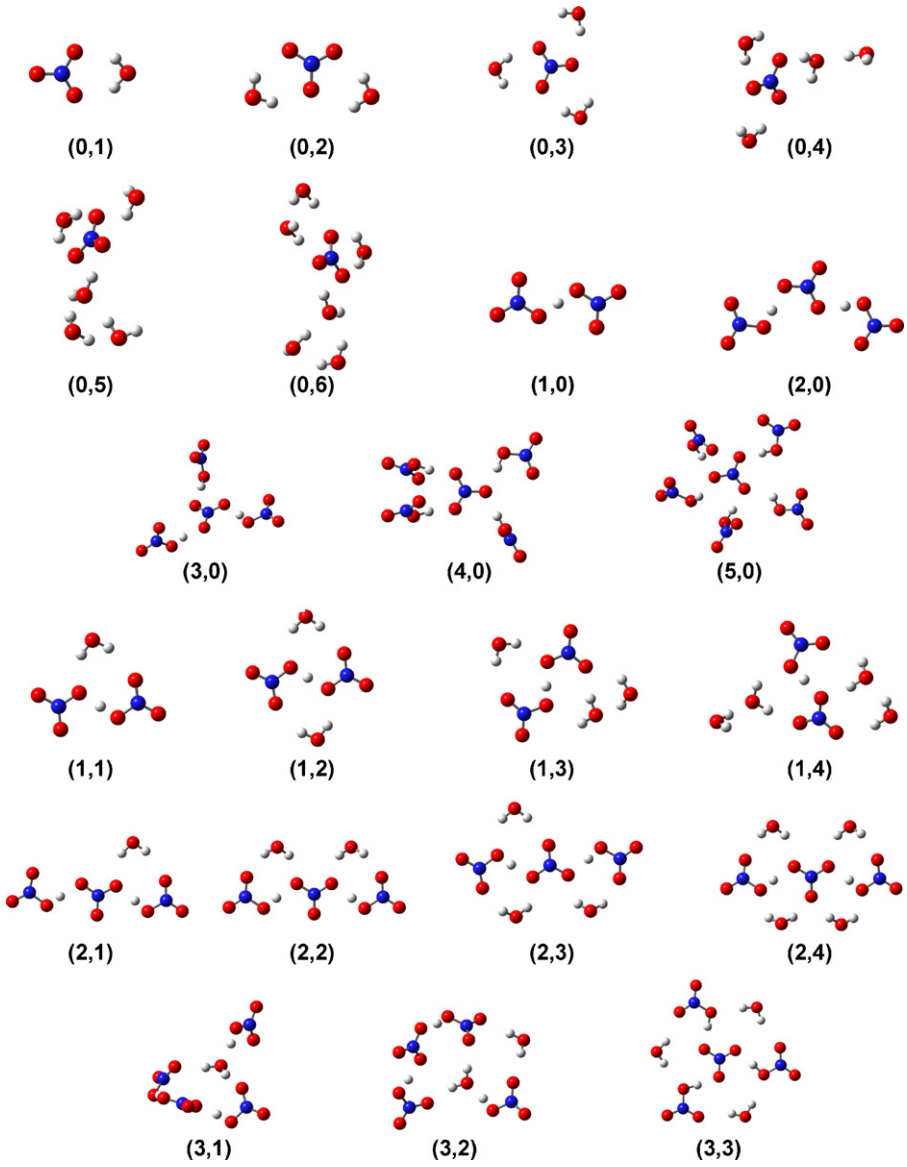

Fig. 8. Possible structures of $NO_3^-(HNO_3)_m(H_2O)_n$ calculated at the B3LYP/6–31++G(d,p) level of theory.

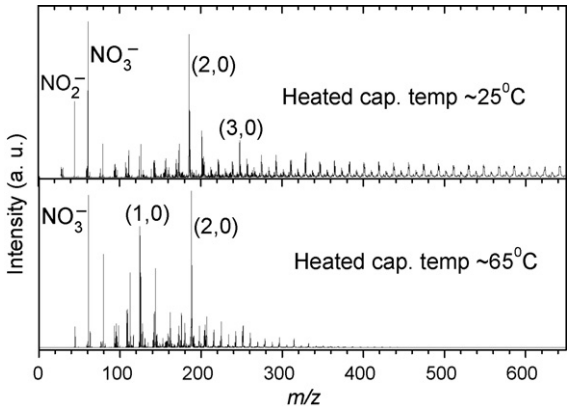

Fig. 9. Negative ion mass spectra obtained with an STM needle at two different heated capillary temperatures.

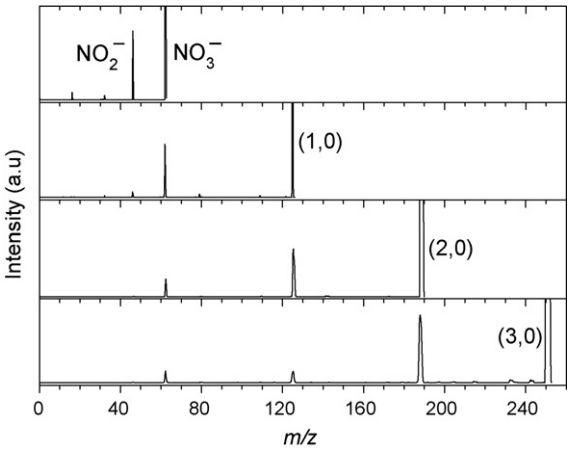

Fig. 11. MIKE spectra obtained after collisions between $NO_3^-(HNO_3)_m$ (m = 0, 1, 2, 3) and Ne. The dominating fragment channel is loss of nitric acid molecules.

second and third nitric acid molecule was found to occur for water clusters with n = 8 and 13 respectively but no clusters with more than three nitric acid molecules were observed in these experiments.

The temperature of the heated capillary has a strong influence on the number of molecules attached to the core ion. The most striking effect observed by raising the temperature from 25 to 65 °C as shown in Fig. 9, is the lack of large water clusters at the higher temperature. This observation can be understood as a result of water evaporation during the passage of the ions through the heated capillary. When the source is used in the ESI mode, the purpose of the capillary is to remove solvent molecules from the analytes.

With our setup it is easy to perform tandem mass spectrometry on selected clusters or core ions. CID-MIKE spectra of what we believe are HCO_3^- and NO_3^- ions are shown in Fig. 10. The negative MIKE spectra only show that we have hydrogen loss in the case of HCO_3^- and that NO_3^- is an ion that contains several oxygen atoms. However, it is also possible to perform charge reversal mass spectrometry where much more detailed information about the molecular composition is obtained. In particular it should be noted that nitrogen ions are also recorded when scanning positive fragments. By combining positive and negative scans an unambiguous identification of the molecular core ions is possible. Examples of MIKE scans involving cluster ions are shown in Fig. 11. The fragmentation channel which by far dominates is loss of HNO_3 from $NO_3^-(HNO_3)_m$ projectiles. An example of CID of a mixed cluster is depicted in Fig. 12. The projectile ion in this case is $NO_3^-(HNO_3)_2(H_2O)_7$. This spectrum shows that the ion fragments by either water loss or by loss of one nitric acid molecule accompanied by water loss. The pure water loss part of the spectrum shows a decreasing likelihood for loss of more molecules, a trend that is normally observed in cluster CID spectra. On the other hand, the peaks associated with loss of one HNO_3 molecule display the opposite trend. Here it is most likely that all seven water molecules are also lost, with a decreasing probability for survival of additional water molecules. These observations are in good agreement with the calculated binding energies for water and nitric acid, respectively (vide supra).

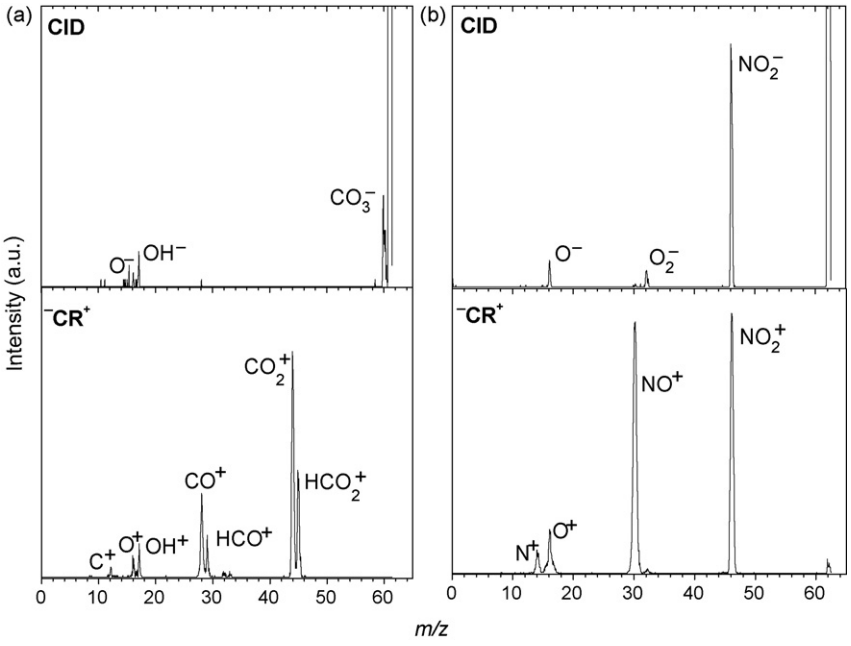

Fig. 10. MIKE spectra obtained after collisions between (a) HCO_3^- or (b) NO_3^- and Ne. In the top panel negative product ions were recorded and in the bottom panel positive ions were recorded.

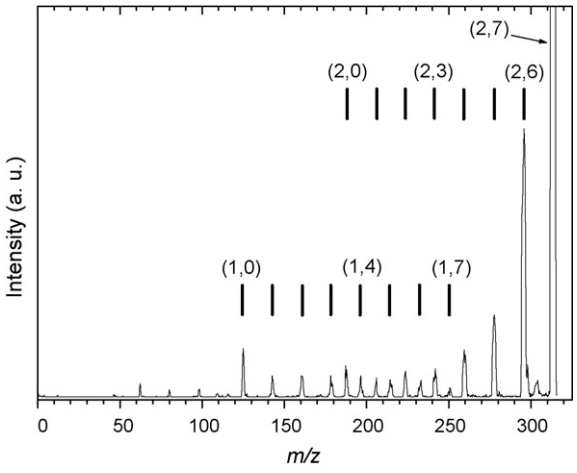

Fig. 12. MIKE spectrum obtained after collisions between $NO_3^-(HNO_3)_2(H_2O)_7$ and Ne. The two fragment series correspond to loss of one or several H_2O molecules and loss of one HNO_3 molecule and one or several H_2O molecules.

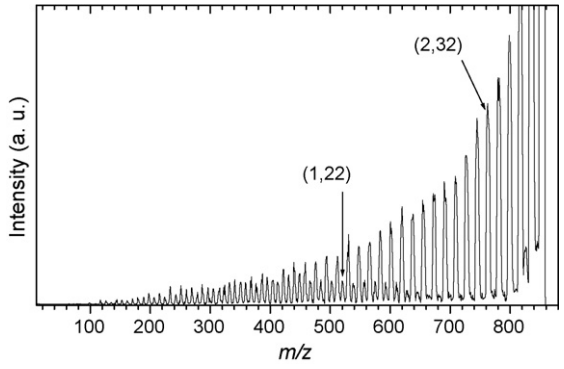

Fig. 13. MIKE spectrum for the precursor ion $NO_3^-(HNO_3)_2(H_2O)_{37}$ with a mass of 854 Da and Ne. The dominating fragment channel is loss of one or several H_2O molecules.

A CID spectrum for $NO_3^-(HNO_3)_2(H_2O)_{37}$ is shown in Fig. 13. Also here water is lost much more readily than nitric acid. The "exponential" fragment distribution is in accordance with the fragment distribution observed earlier for CID of C_{60} [17] and hydrated adenosine 5′-monophosphate nucleotide (AMP) ions [18]. In the case of C_{60} the exponential behavior was explained as a result of sequential evaporation combined with a stop mechanism, healing of a rift in the cage. In the case of $AMP^-(H_2O)_n$ the nearly exponential behavior was explained with a model involving different energy transfers in the collisions resulting in an evaporative ensemble. In the present case the later model seems to be the most plausible since the structures of the clusters presumably are similar.

5. Conclusions

It has been demonstrated that corona discharge in ambient air is able to produce ions with large amounts of water molecules attached, so called aerosols. This is especially so when a very sharp STM needle (high electric field at the needle tip) is applied in the point to plane configuration. The core ions in the aerosol formation process are mainly $NO_3^-(HNO_3)_2$ and $NO_3^-(HNO_3)_3$ and attachment of up to 200 water molecules has been observed. It is most likely that even larger aerosols are produced but for experimental reasons these could not be registered in the present experiment. It is thus demonstrated that one likely route of aerosol formation goes via ion-induced nucleation as suggested by Svensmark et al. [4]. By recording both positive and negative ions after CID it is demonstrated that unambiguous core ion identification can be performed. Dominating fragment channels can be identified from MIKE spectra of mixed cluster ions.

Acknowledgements

We acknowledge Jacques Chevallier for recording the SEM pictures of the corona needle and Erik Lægsgaard for supplying us with the STM needles. This experiment has been performed at ELISA/SEP.1, part of the distributed LEIF infrastructure. The support received by the European Project ITS-LEIF (RII3/026016) is gratefully acknowledged.

References

[1] F. Arnold, Nature 284 (1980) 610.
[2] F. Yu, R.P. Turco, Geophys. Res. Lett. 27 (2000) 883.
[3] F. Yu, R.P. Turco, J. Geophys. Res. 106 (2001) 4797.
[4] H. Svensmark, J.O.P. Pedersen, N.D. Marsh, M.B. Enghoff, U.I. Uggerhøj, Proc. R. Soc. A 463 (2007) 385.
[5] H. Svensmark, Astron. Geophys. 48 (2007) 18.
[6] J.D. Skalny, T. Mikoviny, S. Matejcik, N.J. Mason, Int. J. Mass Spectrom. 233 (2004) 317.
[7] K. Nagato, Y. Matsui, T. Miyata, T. Yamauchi, Int. J. Mass Spectrom. 248 (2006) 142.
[8] K. Sekimoto, M. Takayama, Int. J. Mass Spectrom. 261 (2007) 38.
[9] D. Nna Mvondo, R. Navarro-González, F. Raulin, P. Coll, Origins Life Evol. Biospheres 35 (2005) 401.
[10] O.V. Boltalina, P. Hvelplund, T.J.D. Jørgensen, M.C. Larsen, M.O. Larsson, D.A. Sharoitchenko, M. Sørensen, Phys. Rev. A 62 (2000) 023202.
[11] M.J. Frisch, G.W. Trucks, H.B. Schlegel, G.E. Scuseria, M.A. Robb, J.R. Cheeseman, V.G. Zakrzewski, J.A. Montgomery Jr., R.E. Stratmann, J.C. Burant, S. Dapprich, J.M. Millam, A.D. Daniels, K.N. Kudin, M.C. Strain, O. Farkas, J. Tomasi, V. Barone, M. Cossi, R. Cammi, B. Mennucci, C. Pomelli, C. Adamo, S. Clifford, J. Ochterski, G.A. Petersson, P.Y. Ayala, Q. Cui, K. Morokuma, D.K. Malick, A.D. Rabuck, K. Raghavachari, J.B. Foresman, J. Cioslowski, J.V. Ortiz, A.G. Baboul, B.B. Stefanov, G. Liu, A. Liashenko, P. Piskorz, I. Komaromi, R. Gomperts, R.L. Martin, D.J. Fox, T. Keith, M.A. Al-Laham, C.Y. Peng, A. Nanayakkara, M. Challacombe, P.M.W. Gill, B. Johnson, W. Chen, M.W. Wong, J.L. Andres, C. Gonzalez, M. Head-Gordon, E.S. Replogle, J.A. Pople, Gaussian 98, Revision A.9, Gaussian, Inc., Pittsburgh, PA, 1998.
[12] R. Atkinson, D.L. Baulch, R.A. Cox, J.N. Crowley, R.F. Hampson, R.G. Hynes, M.E. Jenkin, M.J. Rossi, J. Troe, Atmos. Chem. Phys. 4 (2004) 1461.
[13] T. Shindler, C. Berg, G. Niedner-Schatteburg, V.E. Bondybey, J. Chem. Phys. 104 (1996) 3998.
[14] N. Lee, R.G. Keesee, A.W. Castleman Jr., J. Chem. Phys. 72 (1980) 1089.
[15] S. Brøndsted Nielsen, M. Masella, P. Kebarle, J. Phys. Chem. A 103 (1999) 9891.
[16] X. Zhang, E.L. Mereand, A.W. Castleman, J. Phys. Chem. 98 (1994) 3554.
[17] P. Hvelplund, L.H. Andersen, H.K. Haugen, J. Lindhard, D.C. Lorents, R. Malhotra, R. Ruoff, Phys. Rev. Lett. 69 (1992) 1915.
[18] B. Liu, S. Brøndsted Nielsen, P. Hvelplund, H. Zettergren, H. Cederquist, B. Manil, B.A. Huber, Phys. Rev. Lett. 97 (2006) 133401.